Anal Bioanal Chem
DOI 10.1007/s00216-017-0471-y

RESEARCH PAPER

A label-free electrochemical biosensor based on tubulin immobilized on gold nanoparticle/glassy carbon electrode for the determination of vinblastine

Esmaeel Haghshenas[1] · **Tayyebeh Madrakian**[1] · **Abbas Afkhami**[1] · **Haidar Saify Nabiabad**[2]

Received: 5 April 2017 / Revised: 21 May 2017 / Accepted: 14 June 2017

Abstract Vinblastine (VLB) is prescribed for a wide variety of cancers. Therefore, development of sensitive methods for early diagnosis is urgently required. In this work, a highly sensitive and label-free impedimetric biosensor was fabricated for the electrochemical detection of VLB. First, the gold nanoparticles (AuNPs) were electrodeposited on the surface of a glassy carbon electrode (GCE). 3-Mercaptopropionic acid (MPA) was self-assembled over the AuNPs. Then, tubulin (TUB), as a receptor, was covalently immobilized at the AuNPs/GCE surface via carbodiimide coupling reaction using *N*-(3 dimethy laminopropyl)-*N*′-ethyl carbodiimide (EDC) and *N*-hydroxy succinimide (NHS). The step-by-step modification process was characterized by cyclic voltammetry (CV) and electrochemical impedance spectroscopy (EIS) in the presence of a redox probe $[Fe(CN)_6]^{3-/4-}$. The VLB concentration was measured through the increase of impedance values in the corresponding specific binding of VLB and TUB. The increased electron-transfer resistance (R_{et}) values were proportional to the value of VLB concentrations in the range of 0.4 to 65.0 nmol L^{-1} with a detection limit of 8.4×10^{-2} nmol L^{-1} ($SN^{-1} = 3$). The practical analytical performance of the proposed method was demonstrated by determination of VLB in plant extracts and human serum samples with satisfactory recoveries.

Keywords Vinblastine · Tubulin · Biosensor · Impedance spectroscopy · Gold nanoparticle

✉ Tayyebeh Madrakian
madrakian@basu.ac.ir; madrakian@gmail.com

[1] Faculty of Chemistry, Bu-Ali Sina University, Hamedan 6517838695, Iran

[2] Department of Production of Medical Plant, Nahavand University, Nahavand 6591913989, Iran

Introduction

Biosensor-based protocols employing receptor-acceptor interaction is one of the most important analytical techniques in the analytical detection of biomarkers due to the highly specific molecular recognition of biointeraction. In the past decades, many biosensor methods have been reported. But, electrochemical biosensors are especially promising for their indigenous superiority such as low cost, good portability, and high sensitivity [1].

Catharanthus roseus (L.) is a terpenoid indole alkaloid-producing plant that has historically been used to treat a wide assortment of diseases. Because of its therapeutic function as the source of the anticancerous metabolites (such as vinblastine (VLB)), the scientific community is becoming interested in *Catharanthus roseus* [2]. VLB is one of the several tubulin-inhibitor secondary metabolites that have been used for many chemotherapeutic purposes since their introduction in the clinic as antitumour drugs. VLB introduces a wedge at the interface of two tubulin subunits and thus inhibits tubulin assembly [3]. VLB attaches to microtubule ends and detain the dynamic instability of plus tips at the low concentrations [4]. This probably accounts for the cell cycle arrest in cells treated by clinically relevant doses of this drug. When used at much higher concentrations, VLB depolymerizes microtubules, giving rise in particular to protofilament spirals and curls [3]. High concentrations of the drug induce the formation of birefringent paracrystals in the cytoplasm of a variety of cells [5]. In cancer chemotherapy, the normal dose of vinblastine is l–6 mg m^{-2}, resulting in an active serum concentration below 10 ng mL^{-1} several hours after administration. To support pharmacologic and pharmacokinetic investigations, an understanding on drug levels in a target tissue is important; therefore, sensitive, selective,

Published online: 30 June 2017

fast, and reliable bioanalytical methods are essential. Several conventional methods, such as high-pressure liquid chromatography (HPLC) [6, 7], HPLC with electrochemical detection [8–10], LC-MS [11–16], LC-MS-MS [17–19], and electrophoresis [20, 21] have been fabricated to detect VLB in biosamples or pharmaceuticals. Although the mentioned techniques are globally accepted, the sample pretreatment is time consuming and grinding work. Moreover, considerable equipment should be considered. To conquer these weaknesses, electrochemical sensors are used widely for sensitive characteristics such as instrument simplicity, simple pretreatment procedure, small analytical volumes, high sensitivity, and selectivity. Electrochemical methods were reported earlier for VLB determination [22, 23], but there are no reports about the application of electrochemical biosensors for it. Therefore, the detection of VLB in serum is crucial for an effective early diagnosis and very helpful for further treatments.

In the past decade, nanoparticles (NPs) are widely used in biosensors due to their unique electronic, optical, and mechanic properties. Various NPs such as silver, gold, quantum dots, and silica have been applied for ultrasensitive electrochemical and optical bioassays. For many years, gold nanoparticles (AuNPs) have been used for bioanalytical methods due to the following advantages: fast and simple synthesis, a narrow size distribution, fascinating electronic and optical characteristics, and efficient coating by thiols or other biomolecules. These characteristics of gold NPs make them an ideal option for the immobilization of biomolecules for biosensing. Further, the electrochemical properties of gold NPs show that they have interesting properties by facilitating electron transfer, improving the electrode conductivity, and the detection limit of biomolecules. Moreover, gold NPs can provide a stable surface for the immobilization of biomolecules, such that the molecules retain their biological activities [24–28].

In the present study, we reported for the first time an electrochemical biosensor for VLB detection through the use of immobilized TUB on gold nanoparticle-modified glassy carbon electrode (AuNPs/GCE). A GCE was electrochemically modified with AuNPs, and then TUB is covalently attached to the AuNP-coated surface (AuNPs/GCE) by using 3-mercaptopropionic acid (MPA) via the formation of a stable self-assembled monolayer (SAM). Electrochemical impedance spectroscopy (EIS) and cyclic voltammetry (CV) were applied to investigate the fabrication process of modified electrode and determination of VLB. After immobilization of TUB on the modified electrode, the detection of VLB was realized by monitoring the changes in the electron transfer kinetics and diffusion of the electrochemical probe ($[Fe(CN)_6]^{3-/4-}$). This work constitutes the first application of TUB as a receptor in the field of electrochemical biosensors. The biosensor was used to analyze VLB in human serum samples.

Experimental

Reagents and apparatus

VLB was purchased from Tocris Bioscience (UK), tubulin (TUB) was purchased from SignalChem (USA), chloroauric acid ($HAuCl_4$, $4H_2O$) was obtained from Sigma-Aldrich (USA), and other chemicals and solvents used were of analytical reagent grade and used directly without further purification. All solutions were prepared by double-distilled water (DDW). Phosphate buffer solution (PBS) with pH 7.4 was used for all electrochemical measurements.

CV and EIS were carried out on potentiostat/galvanostat (Autolab PGSTAT302 N). A conventional three-electrode system was used for the electrochemical investigations, which comprised a silver/silver chloride (KCl) as the reference electrode, a platinum wire as the auxiliary electrode, and a T/MPA/AuNPs/GCE as the working electrode. Metrohm pH meter (Model 713) with a glass electrode was used to adjust the pH of solutions. The morphology of bare and modified GCE was investigated by using a scanning electron microscope (SEM, MIRA3 TESCAN).

The EIS was collected in frequency range of 0.1 to 100 kHz. The Commercial software Nova version 1.7 was used to fit the data from Nyquist plot. To understand the surface structure, impedance data was fit from equivalent circuit.

Preparation of gold nanoparticles/glassy carbon electrode

The surface of GCE was polished successively with 0.3 μm Al_2O_3 water slurry using a polishing cloth, and it was rinsed with DDW. The polished electrode was sonicated subsequently in a 1:1 aqueous HNO_3 solution, ethanol, and DDW each for 10 min, to remove all contaminants that may be on the electrode surface. The pretreated electrode was immersed into a solution containing 3.0 mmol L^{-1} $HAuCl_4$ and 0.5 mol L^{-1} H_2SO_4, and the gold nanoparticles were electrodeposited at −0.2 V for 220 s [29–32]. The modified electrode (AuNPs/GCE) was taken out and rinsed with DDW.

The effective surface area (A) for GCE and AuNPs/GCE was determined from cyclic voltammograms of 1.0 mmol L^{-1} $[Fe(CN)_6]^{3-/4-}$ in 0.1 M KCl solution. For a reversible process, the peak current i_p is linearly proportional to $\nu^{1/2}$ as follows:

$$i_p = \left(2.69 \times 10^5\right) n^{3/2} A C D^{1/2} \nu^{1/2} \quad (1)$$

where i_p is the peak current, n is the number of electrons in the reaction, A is the electrode area, D is the diffusion coefficient of $[Fe(CN)_6]^{3-/4-}$ ($D = 7.60 \times 10^{-6}$ cm^2 s^{-1}) [33], C is the concentration of $[Fe(CN)_6]^{3-/4-}$, and ν is the scan rate. From the slope of the i_p vs. $\nu^{1/2}$ line, the values of A were determined as 0.061 and 0.089 cm^2 for GCE and AuNPs/GCE,

respectively. Therefore, modification of GCE by AuNPs causes the electroactive surface area to increase (~1.46-fold), indicating that the introduction of the AuNPs provides more conduction pathways for the electron transfer of $[Fe(CN)_6]^{3-/4-}$.

Fabrication of the biosensor

The AuNPs/GCE was immersed in MPA solution (50 mmol L^{-1}) for 3 h at room temperature. At this step, self-assembled monolayers of 3-mercaptopropionic acid (MPA) were formed. Then, the modified electrode was washed with water to remove MPA residues and drying. The terminal carboxylic groups of MPA-modified electrode (MPA/AuNPs/GCE) were then activated by immersing the electrodes in PBS (pH = 5.5) containing 2.0 mmol L^{-1} EDC and 5.0 mmol L^{-1} NHS for 2 h [34, 35]. Then, the electrode was rinsed using the PBS and immediately immersed in 0.2 mg mL^{-1} TUB in PBS (pH 7.4) for 2 h to fabricate T/MPA/AuNPs/GCE. Then the electrodes were washed several times with PBS (pH 7.4) to remove unbound TUB and used for electrochemical measurements. The designed biosensor was stored at 4 °C when not in use.

Electrochemical impedance spectroscopy and cyclic voltammetry

The prepared VLB biosensor was incubated in a solution containing different concentrations of VLB for 25 min and washed carefully with PBS. The electrochemical measurements including CV and EIS were performed in a degassed PBS solution containing 0.1 mol L^{-1} KCl and 2.0 mmol L^{-1} $[Fe(CN)_6]^{3-/4-}$. The stepwise sensor fabrication process and the formation of VLB-TUB bind is shown in Scheme 1.

Real-sample preparation

Serum sample preparation

Drug-free serum samples that were taken from Bessat Hospital (Hamedan, Iran) were collected from healthy donors with informed consent. All the experiments were performed in compliance with the relevant laws and institutional guidelines. For preparation of serum sample, 1.0 mL of serum was diluted to 100.0 mL by PBS (pH 7.4). Then, 25 mL of this solution was transferred to the voltammetric cell and different amounts of VLB were added and the recovery percent was obtained by EIS technique.

Preparation of the plant extracts

Dried plants (*C. roseus*) were powdered by a cylindrical crusher. Ethanolic, aqueous, and methanolic extracts were prepared by maceration method [36]. About 20 g of dried powder was separately added to 100 mL of ethanol and placed on a shaker for 72 h. The extracts were filtered through filter paper and centrifuged at 10,000 rpm for 10 min, then concentrated by the rotary and the extracts transferred to oven at 40 °C to be dried. The residues were stored in a dark glass bottle at −22 °C freezer and used for the next analysis.

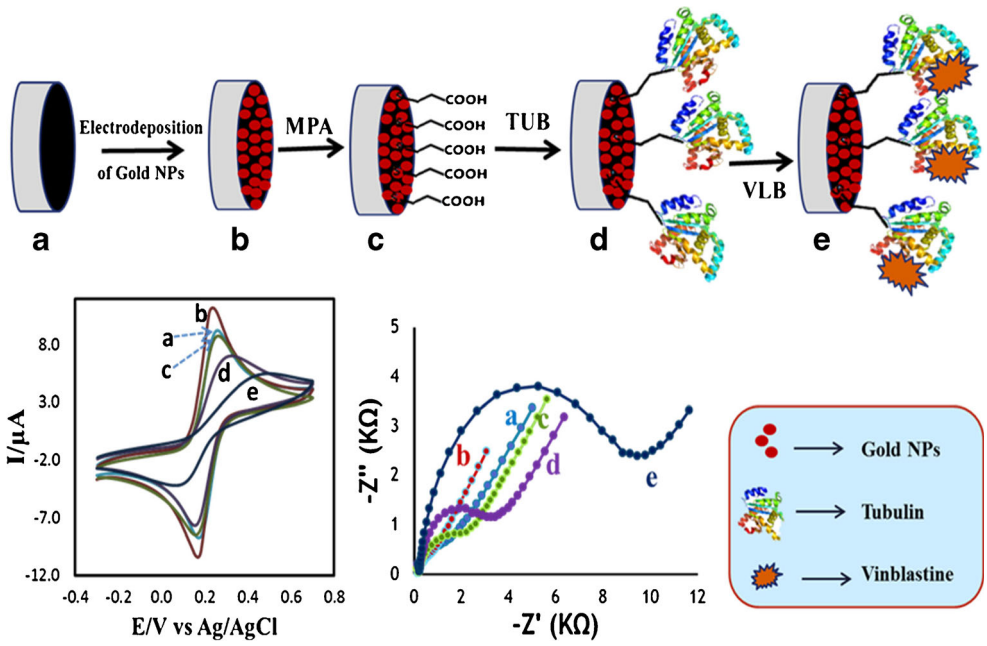

Scheme 1 The fabrication steps of the designed biosensor for the determination of VLB

Results and discussion

Characterization of the developed biosensor

The AuNPs/GCE was characterized using CV and EDS. Figure 1A shows cyclic voltammograms of GCE and AuNPs/GCE in PBS (pH = 7.0) at a scan rate of 50 mV s^{-1}. There is no oxidation or reduction peaks potentially from −0.7 to 1.3 V vs. Ag/AgCl at GCE. But, the peaks were observed at 0.9, 0.46, and −0.23 V on AuNPs/GCE. These peaks related to oxidation (0.9 V) and reduction (0.46 and −0.23 V) of AuNPs. The results indicate that the AuNPs were electrodeposited on GCE.

In order to have more information about the AuNPs/GCE surface, the EDS pattern was obtained. As shown in Fig. 1B, EDS spectrum confirms the presence of Au on the GCE surface.

The SEM was used for characterize morphologies of AuNPs electrodeposited on the GCE. The SEM image in Fig. 2A indicates that an appropriate layer of AuNPs with small particle size is formed on the surface of the GCE. As seen, AuNPs were homogeneously deposited on the surface of the GCE which were well dispersed without aggregation. However, the SEM image of T/MPA/AuNPs/GCE is shown in Fig. 2B. AuNPs were clearly surrounded by a blurry film, which was caused by the immobilization of protein, TUB, over the AuNP-modified matrix.

Electrochemical behaviors of the biosensor

Preparation process of the T/MPA/AuNPs/GCE was characterized by EIS and CV. All electrochemical analysis were carry out in PBS solution, pH 7.4, containing 0.1 mol L^{-1} KCl and 2.0 mmol L^{-1} $[Fe(CN)_6]^{3-/4-}$. The $[Fe(CN)_6]^{3-/4-}$ probe was applied as a probe to study the changes in electrode behavior after each electrode-modification step. The changes in the separation peak potentials of and peak current in CV, at the surface of different electrodes are theoretically associated with the electron transfer rate constant, i.e., the electron transfer resistance [37]. Figure 3 shows the CVs of $[Fe(CN)_6]^{3-/4-}$ at the bare GCE (curve a), AuNPs/GCE (curve b), MPA/AuNPs/GCE (curve c), T/MPA/AuNPs/GCE (curve d), and VLB-combined T/MPA/AuNPs/GCE (curve e), respectively. As shown in Fig. 3, when AuNPs are deposited on the GCE (curve b), the peak current of $[Fe(CN)_6]^{3-/4-}$ was increased compared with that of the GCE, indicating that the introduction of the AuNPs played a role in the increase of the electroactive surface area. The peak separation potentials were decreased, indicating that the AuNPs on GCE promote the electron transfer between the $[Fe(CN)_6]^{3-/4-}$ and the electrode surface [38, 39]. Other stepwise modification on the T/MPA/AuNPs/GCE was accompanied by a decrease in the current response and an increase in the peak-to-peak separation potentials between the anodic and cathodic peaks of the redox probe, displaying that the electron-transfer kinetics of $[Fe(CN)_6]^{3-/4-}$ is obstructed. After the AuNPs/GCE was functionalized with MPA, the electron transfer between $[Fe(CN)_6]^{3-/4-}$ and electrode surface was inhibited. When TUB were immobilized on the electrode surface, the peak currents of the redox probe of $[Fe(CN)_6]^{3-/4-}$ decreased again. In particular, after VLB molecules were combined with the TUB molecules, an obvious disappearance of the anodic and cathodic peaks was observed (curve e).

The spectra of impedance include a linear and a semicircle part. The semicircle and the linear parts related to the electron transfer-limited process and the diffusion process, respectively. The semicircle diameter values are symmetric to the electron-transfer resistance (R_{et}) [40]. Figure 3B shows the Nyquist plots of different modification steps of electrode in $[Fe(CN)_6]^{3-/4-}$ solution. A very small semicircle portion was recorded for the bare GCE (curve a), which indicated a rapid electron transfer process. The semicircle diameter was

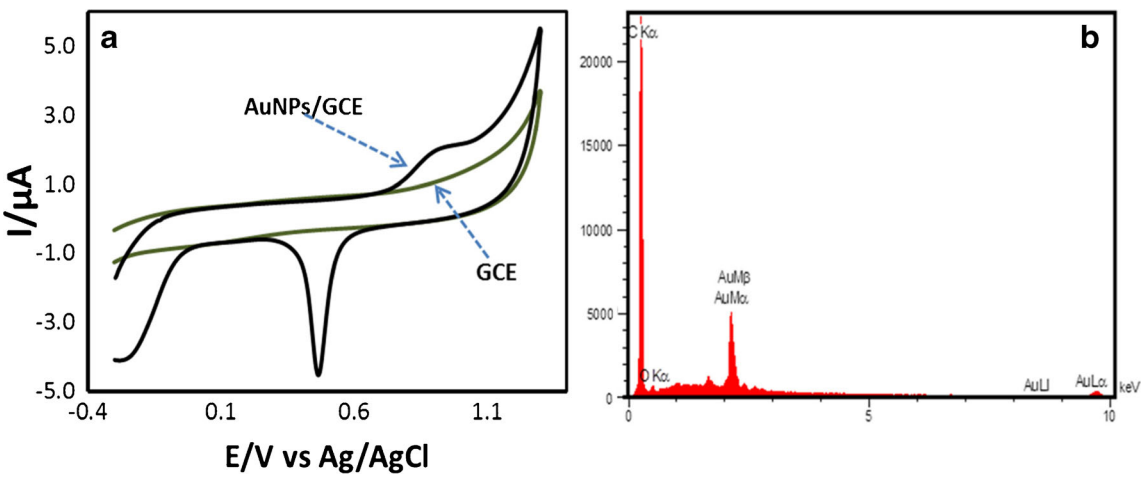

Fig. 1 **A** CVs of GCE and AuNPs/GCE in PBS (pH = 7.0) at a scan rate of 50 mV s^{-1}; **B** EDS spectrum of the AuNPs/GCE

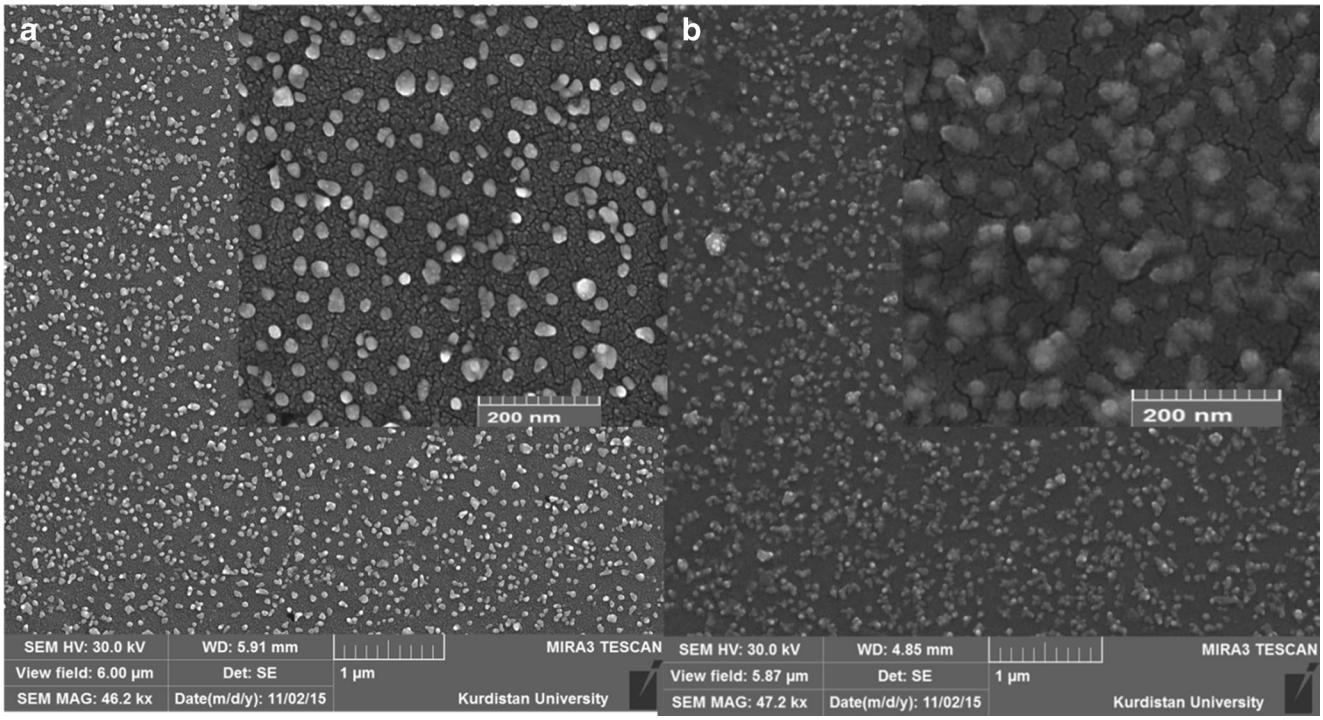

Fig. 2 SEM images of **A** AuNPs/GCE and **B** T/MPA/AuNPs/GCE

decreased after the electrodeposition of AuNPs to the surface of GCE (curve b). The presence of the AuNP layer on the GCE increases the surface area of electrode and led to the significant acceleration of the electron transfer. Furthermore, AuNPs on the GCE provided a specific platform for increased loading of TUB via the linker agent. In the next step, the MPA as linker agent was added to the AuNPs/GCE. In this step, the semicircle diameter became bigger and consequently electron transfer resistance was increased (curve c). However, after TUB was assembled on the AuNPs/GCE surface, an apparent increase of the semicircle diameter was also observed (curve d). The result indicated that the TUB layer on the electrode generated a barrier for electron transfer. When the T/MPA/AuNPs/GCE was incubated with the 4.0-nmol L^{-1} VLB solution, the impedance increased dramatically (curve e). This was mainly attributed to the fact that the formation of VLB-TUB complex on the electrode surface further blocks the electron transfer process. These above EIS results vividly indicated that the biosensor was successfully constructed, and the changing of the impedance spectra caused by analyte may be employed to the detection of VLB.

In order to fit the obtained impedance data in the experiment, the Randles circuit was chosen. The value of R_{et} depends on the insulating and dielectric features at the electrode/electrolyte interface, which can be estimated from the diameter of the semicircle of the Nyquist plots. By fitting the data, R_{et} was estimated to be 839, 334, 1230, and 2500 Ω at the GCE, AuNPs/GCE, MPA/AuNPs/GCE, and T/MPA/

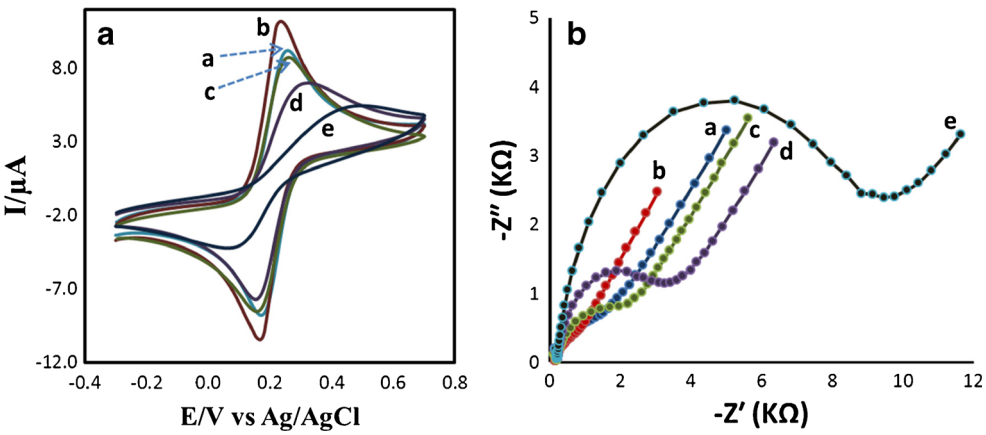

Fig. 3 **A** Cyclic voltammograms and **B** Nyquist plots of *a* bare GCE, *b* AuNPs/GCE, *c* MPA/AuNPs/GCE, *d* T/MPA/AuNPs/GCE, and *e* T/MPA/AuNPs/GCE incubated with 4.0 nmol L^{-1} VLB in 0.1 mol L^{-1} PBS (pH = 7.4) containing 0.1 mol L^{-1} KCl and 2.0 mmol L^{-1} $[Fe(CN)_6]^{3-/4-}$

AuNPs/GCE, respectively. Finally, after incubating with the 4.0-nmol L^{-1} VLB, the R_{et} increased dramatically to 6194 Ω.

Optimization of the experimental conditions of the biosensor

For the best analytical performance of the developed biosensor, several experimental parameters (TUB concentration, pH, the binding time, and the incubation time) were optimized.

Optimization of TUB concentration

The influence of TUB concentration on the EIS responses of T/MPA/AuNPs/GCE was investigated, which was very essential to the sensitivity of the sensor. As shown in Fig. 4A, the R_{et} of the T/MPA/AuNPs/GCE increased gradually with the increasing of TUB amounts, and the R_{et} value was inclined to best able when the TUB concentration was 0.1 mg mL^{-1}. Therefore, 0.1 mg mL^{-1} was selected as the optimal TUB concentration for the biosensor construction in this experiment.

Optimization of binding time

The reaction time between TUB and activated MPA/AuNPs/GCE was optimized (Fig. 4B), and it was obvious that the R_{et} of the modified electrode increased with the growth of the interaction time from 20 to 120 min and then reached a maximum value in 120 min. Hence, 120 min reaction time was selected as the reaction time in the following experiment.

Optimization of pH

The effect of pH on the designed biosensor response was investigated. The response of biosensor for 5.0 nmol L^{-1} VLB in PBS with different pH values was evaluated by recording R_{et}. As shown in Fig. 4C, the R_{et} increases with increasing of pH value from 4.0 to 7.4 and decreases when pH value increases further. Since maximum ΔR_{et} occurs at pH 7.4, this value was chosen as the optimum value for VLB measurement.

Optimization of incubation time

Incubation time for the formation VLB-TUB complex was another important factor to affect the sensitivity of the biosensor. So, the effect of the incubation time on the developed biosensor was investigated. For this purpose, the T/MPA/AuNPs/GCE was incubated for different times (5–50 min) in the presence of VLB (5.0 nmol L^{-1}). As shown in Fig. 4D, the biosensor response increased with increasing incubation time between 5 and 25 min and then reached to level off after 25 min. Therefore, 25 min was enough incubation time for measuring of VLB in a proposed sensor.

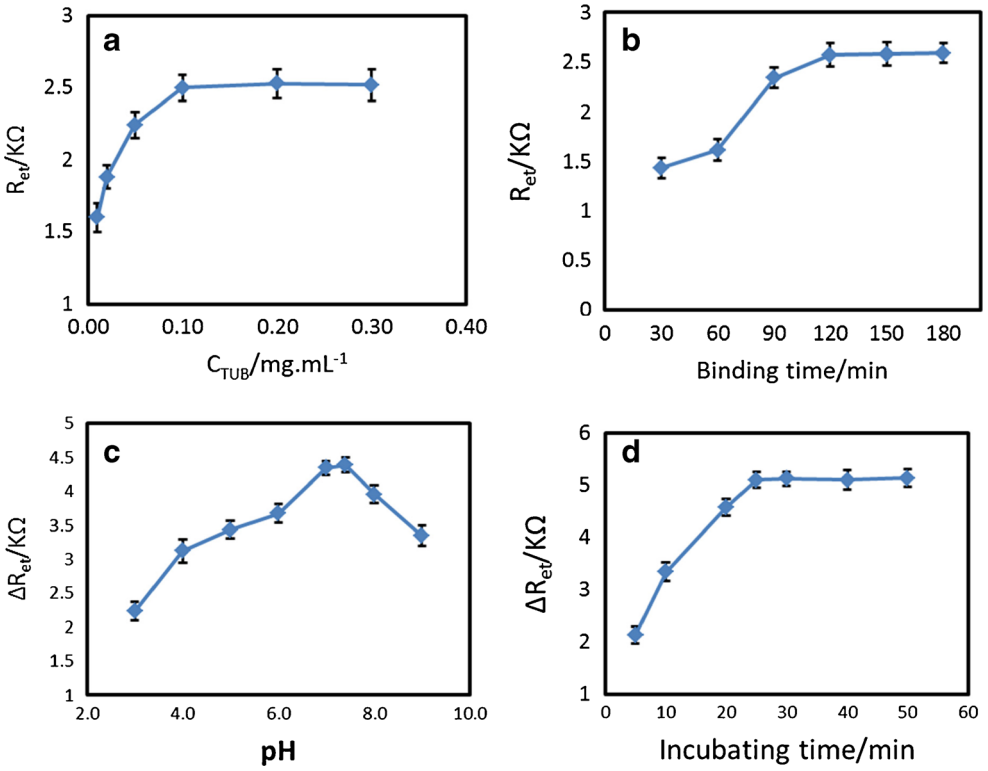

Fig. 4 Effects of **A** the TUB concentration, **B** the binding time between TUB and MPA/AuNPs/GCE, **C** solution pH value, and **D** incubating time of 5.0 nmol L^{-1} VLB with TUB on the EIS responses of T/MPA/AuNPs/GCE

Electrochemical impedance spectroscopy for the detection of VLB

At the optimal experimental conditions, the EIS responses of T/MPA/AuNPs/GCE for the determination of different VLB concentrations were obtained. An impedance data for sample solution containing no VLB at T/MPA/AuNPs/GCE, and the R_{et} obtained was taken as a blank sample response. Subsequently, R_{et} was measured for the detection of VLB-TUB interaction after each addition of aliquots of different concentrations of VLB solution. Figure 5A shows the Nyquist plots of impedance spectra for the different concentrations of VLB solution at the T/MPA/AuNPs/GCE. As shown in Fig. 5A, the diameter of Nyquist circle increased with increasing concentration of added VLB, demonstrating VLB-TUB interaction, at the electrode surface. The interaction between VLB and TUB acts as a kinetic barrier for the electron transfer at the interface of electrode surface, resulting in a corresponding increase in R_{et}.

The calibration plot is shown in Fig. 5B. It relates to the electron transfer resistance at the sensing interface with different concentrations of VLB. The change of R_{et} is calculated following the equation:

$$\Delta R_{et} = R_{et\ (TUB-VLB)} - R_{et\ (TUB)} \quad (2)$$

where $R_{et\ (TUB-VLB)}$ is the value of the electron transfer resistance after VLB binding to TUB, $R_{et\ (TUB)}$ is the value of the electron transfer resistance of blank (as TUB immobilized on the MPA/AuNPs/GCE). The electron transfer resistances are proportional to the VLB concentrations in two linear ranges. For lower concentration range that is from 0.4 to 12.0 nmol L^{-1} with a calibration equation of ΔR (KΩ) = 0.9083 C (nmol L^{-1}) + 0.6441 (R^2 = 0.9910), whereas for higher concentration range (12.0–65.0 nmol L^{-1}), with a calibration equation of ΔR (KΩ) = 0.1885 C (nmol L^{-1}) + 9.3462 (R^2 = 0.9909). These two linear ranges with different slopes can be due to the fact that the amount of tubulin immobilized on the modified electrode surface is somewhat certain. When the biosensor was applied to determination of low VLB concentrations, VLB molecules can readily attached with the abundant active sites of tubulin present on the modified electrode surface. When the concentration of VLB increased, the active sites of tubulin available on the modified electrode surface for attaching with VLB become fewer. Therefore, the sensitivity (slope) declines when the biosensor is used to determine higher concentrations of VLB and two linear ranges with different slopes are observed. The detection limit was found to be 8.4×10^{-2} nmol L^{-1} at a signal to noise of 3.

Selectivity, reproducibility, and stability of the biosensor

The selectivity of the biosensor for analysis of biological samples without any separation step is an important parameter. In order to study the binding selectivity of the biosensor toward VLB, control experiments were performed under the same experimental conditions. The influence of some common ions and organics on the detection of VLB was studied. It was found that the 500 times of concentration of Ca^{2+}, Na^{+}, Cu^{2+}, Zn^{2+} Cl^{-}, SO_4^{2-}, glucose, and citric acid, 100 times of tyrosine and tryptophan, and 50 times of uric acid and ascorbic acid, did not affect the detection of VLB (signal variation <5%). The interference of some proteins (such as hemoglobin (HG) and bovine serum albumin (BSA)) and some compounds with similar structure (such as vincristine, vinorelbine, and vindesine) were also investigated. The results show that the 100 times BSA and HG did not cause the significant change in the signal of VLB. In the case of vincristine, vinorelbine, and vindesine, two or three times of concentration of these compounds have interference to determine VLB. But, due to the fact that these compounds do not exist with VLB in the real samples, they do not have an interference to determine VLB. It suggests that the selectivity of the biosensor was acceptable.

The reproducibility of the biosensor was evaluated by fabricating five independent modified electrodes at the

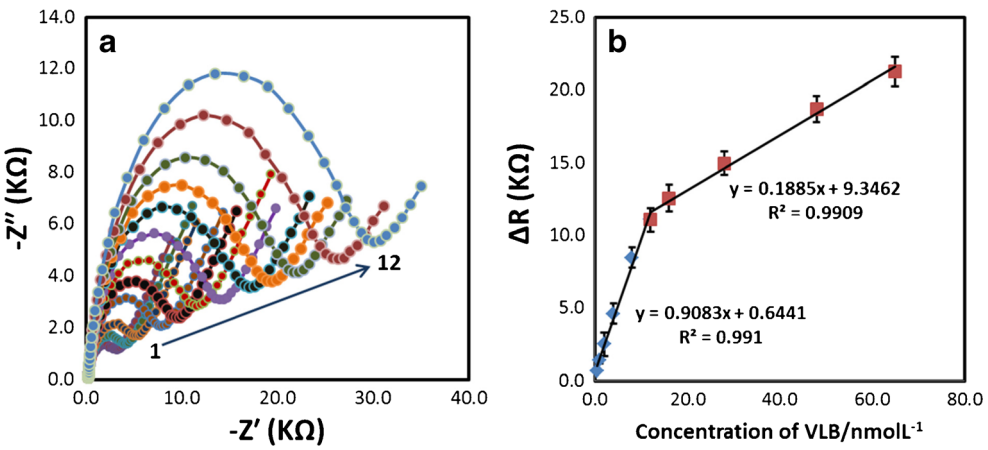

Fig. 5 **A** EIS responses of the T/MPA/AuNPs/GCE for the detection of VLB with different concentrations (from 1 to 12: 0, 0.4, 1.0, 2.0, 4.0, 8.0, 12.0, 16.0, 28.0, 48.0, and 65.0 nmol L^{-1}) in 0.1 mol L^{-1} PBS containing 2.0 mmol L^{-1} $[Fe(CN)_6]^{3-/4-}$ and 0.1 mol L^{-1} KCl; **B** the calibration curve for VLB determination

identical experimental condition and using them for the detection of 5.0 nmol L^{-1} VLB. The relative standard deviation was 3.2%. These results indicate acceptable reproducibility and precision of the proposed bioassay.

In addition, the stability of the biosensor was also studied by testing impedimetric response over 20 days of storage at 4 °C. No significant change in impedimetric response was found during 20 days. The biosensor retained 98, 96, and 91% of its initial response after 5, 10, and 20 days of storage, respectively, indicating a good stability of the biosensor.

VLB determination in real samples

In order to evaluate the feasibility of the developed bioassay for real-sample analysis, the biosensor was used for the determination of VLB in plant extracts and serum samples. Serum sample was obtained from an apparently healthy male volunteer with informed consent, and all experiments were performed in compliance with the relevant laws and institutional guidelines. After sample preparation and adequate dilution steps as described earlier, the EIS method was applied to the determination of VLB in plant extracts and serum samples. The summarized results for the analysis are presented in Table 1. The VLB concentration was determined from a calibration curve by averaging five repeated measurements. The detection results showed that the recoveries were from 97.2 to 104.0%, and the relative standard deviations were from 2.9 to 4.1%, so the proposed biosensor can be used in clinical purposes.

The comparison of the results for the determination of VLB by different methods and different analytical parameters in the literature [12, 14, 17, 18, 20, 21, 41] is given in Table 2. Comparing of data suggested priority of the fabricated biosensor over some earlier methods reported in literature, especially for the detection limit.

Table 1 Determination results of VLB in plant extract and serum samples ($n = 5$)

Sample	Added (nmol L^{-1})	Found (nmol L^{-1})	Recovery %	RSD %
Serum	–	ND	ND	–
	5.0	5.2	104.0	3.8
	30.0	29.3	97.7	3.2
Plant extraction	–	22.3	–	2.9
	10.0	31.4	97.2	4.1
	30.0	54.1	103.4	3.3

ND not detected

Table 2 Comparison of the analytical performance of different methods for determination of VLB

Method	Linear range (nmol L^{-1})	Detection limit (nmol L^{-1})	Real sample	Ref.
LC-MS	12.3–1233	2.5	Plasma	[12]
LC-MS	1.2–616.5	0.37	Tumor tissue	[14]
LC-MS-MS	1.85–1926.6	0.92	*Catharanthus roseus*	[17]
LC-MS-MS	0.15–123.3 1.23–2466	0.15 0.15	Plasma Urine	[18]
CE-MS	3.0–148.0	0.99	Catharanthus roseus	[20]
Electrophoresis	18.5–2466	18.5	Plasma	[21]
Flow-injection	0.25–6.17	0.25	Catharanthus roseus	[41]
Electrochemical biosensor	0.4–65.0	0.084	Catharanthus roseus and serum	This work

CE-MS capillary electrophoresis-mass spectrometry, *LC-MS* liquid chromatography-mass spectrometry

Conclusions

The present work describes a new approach for the fabrication of a VLB biosensor based on the covalent immobilization of a TUB on a MPA self-assembled monolayer (as linker) formed on AuNPs which were electrochemically deposited onto a GCE surface. In order to characterize the individual steps involved in the fabrication of the T/MPA/AuNPs/GCE and VLB-TUB interaction at the electrode surface, the cyclic voltammetry and impedance spectroscopic techniques were used. A linear relationship between the electron-transfer resistance and VLB concentration was found in the range of 0.4 to 65.0 nmol L^{-1} with a detection limit of 8.4×10^{-2} nmol L^{-1}. Results show that the biosensor has a wide linear range, high sensitivity, acceptable stability, and good selectivity and reproducibility. Thus, the proposed biosensor and its fabrication procedure may provide a potential application for the detection of VLB in clinical diagnosis.

Acknowledgments The authors acknowledge the Bu-Ali Sina University Research Council and Center of Excellence in Department of Environmentally Friendly Methods for Chemical Synthesis (CEDEFMCS) for providing support to this work.

Compliance with ethical standards

Conflict of interest The authors declare that they have no competing interest.

References

1. Fang Y, Huang X, Zeng Q, Wang L. Metallic nanocrystallites-incorporated ordered mesoporous carbon as labels for a sensitive simultaneous multianalyte electrochemical immunoassay. Biosens Bioelectron. 2015;73:71–8.
2. Mu F, Yang L, Wang W, Luo M, Fu Y, Guo X, et al. Negative-pressure cavitation extraction of four main vinca alkaloids from *Catharanthus roseus* leaves. Molecules. 2012;17:8742–52.
3. Gigant B, Wang C, Ravelli RBG, Roussi F, Steinmetz MO, Curmi PA, et al. Structural basis for the regulation of tubulin by vinblastine. Nature. 2005;435:519–22.
4. Jordan MA, Wilson L. Microtubules as a target for anticancer drugs. Nature Rev Cancer. 2004;4:253–65.
5. Nogales E, Medrano FJ, Diakun GP, Mant GR, Towns-Andrews E, Bordas J. The effect of temperature on the structure of vinblastine-induced polymers of purified tubulin: detection of a reversible conformational change. J Mol Biol. 1995;254:416–30.
6. Gupta MM, Singh DV, Tripathi AK, Pandey R, Verma RK, Singh S, et al. Simultaneous determination of vincristine, vinblastine, catharanthine, and vindoline in leaves of *Catharanthus roseus* by high-performance liquid chromatography. J Chromatogr Sci. 2005;43:450–3.
7. Tikhomiroff C, Jolicoeur M. Screening of *Catharanthus roseus* secondary metabolites by high-performance liquid chromatography. J Chromatogr A. 2002;955:87–93.
8. Vendrig DEMM, Holthuis JJM. Solid-phase extraction of vinblastine and vincristine from plasma and urine: variable drug recoveries due to non-reproducible column packings. J Chromatogr B Biomed Sci Appl. 1987;414:91–100.
9. Ranta Y-P, Callaway JE, Naaranlahti T. Electrochemical detection of alkaloids in HPLC. Mod Method Plant Anal. 1994;15:91–114.
10. Singh DV, Maithy A, Verma RK, Gupta MM, Kumar S. Simultaneous determination of catharanthus alkaloids using reversed phase high performance liquid chromatography. J Liq Chromatogr Relat Tech. 2000;23:601–7.
11. Drapeau D, Blanch HW, Wilke CR. Liquid chromatographic isolation of vincristine and vinblastine. J Chromatogr A. 1987;390:297–306.
12. Gao S, Zhou J, Zhang F, Miao H, Yun Y, Feng J, et al. Rapid and sensitive liquid chromatography coupled with electrospray ionization tandem mass spectrometry method for the analysis of paclitaxel, docetaxel, vinblastine, and vinorelbine in human plasma. Ther Drug Monit. 2014;36:394–400.
13. Zhou H, Tai Y, Sun C, Pan Y. Rapid identification of vinca alkaloids by direct-injection electrospray ionisation tandem mass spectrometry and confirmation by high-performance liquid chromatography–mass spectrometry. Phytochem Anal. 2005;16:328–33.
14. Kosjek T, Dolinšek T, Gramec D, Heath E, Strojan P, Serša G, et al. Determination of vinblastine in tumour tissue with liquid chromatography–high resolution mass spectrometry. Talanta. 2013;116:887–93.
15. Chen Q, Zhang W, Zhang Y, Chen J, Chen Z. Identification and quantification of active alkaloids in *Catharanthus roseus* by liquid chromatography–ion trap mass spectrometry. Food Chem. 2013;139:845–52.
16. Damen CWN, Rosing H, Schellens JHM, Beijnen JH. High-performance liquid chromatography coupled with mass spectrometry for the quantitative analysis of vinca-alkaloids in biological matrices: a concise survey from the literature. Biomed Chromatogr. 2010;24:83–90.
17. Lin Z, Qing-Hui G, Yuan-Gang Z, Lei Y, Yu-Liang M, Yang L. Simultaneous quantitative determination of five alkaloids in *Catharanthus roseus* by HPLC-ESI-MS/MS. Chin J Nat Med. 2014;12:786–93.
18. Achanta S, Ngo M, Veitenheimer A, Maxwell LK, Wagner JR. Simultaneous quantification of vinblastine and desacetylvinblastine concentrations in canine plasma and urine samples using LC–APCI–MS/MS. J Chromatogr B. 2013;913:147–54.
19. Ferreres F, Pereira DM, Valentão P, Oliveira JMA, Faria J, Gaspar L, et al. J Pharm Biomed Anal. 2010;51:65–9.
20. Chen Q, Li N, Zhang W, Chen J, Chen Z. Simultaneous determination of vinblastine and its monomeric precursors vindoline and catharanthine in *Catharanthus roseus* by capillary electrophoresis–mass spectrometry. J Sep Sci. 2011;34:2885–92.
21. Sidorova AA, Yaroshenko DV, Murashko EA, Grigor'ev AV. Development of chromatographic and electrophoretic ethods for determining vinblastine in blood plasma and prostate gland tissue. J Anal Chem. 2013;68:265–71.
22. Temizer A. Electroanalytical determination of vinca alkaloids used in cancer chemotherapy. Talanta. 1986;33:791–4.
23. Haque IU, Saba H. Voltammetry of an anti-cancer drug. ECS Trans. 2009;16:3–23.
24. Ding C, Li H, Hu K, Lin JM. Electrochemical immunoassay of hepatitis B surface antigen by the amplification of gold nanoparticles based on the nanoporous gold electrode. Talanta. 2010;80:1385–91.
25. Madrakian T, Haghshenas E, Afkhami A. Simultaneous determination of tyrosine, acetaminophen and ascorbicacid using gold nanoparticles/multiwalled carbon nanotube/glassy carbon electrode by differential pulse voltammetric method. Sens Actuat B Chem. 2014;193:451–60.
26. Tang H, Chen J, Nie L, Kuang Y, Yao S. A label-free electrochemical immunoassay for carcinoembryonic antigen (CEA) based on gold nanoparticles (AuNPs) and nonconductive polymer film. Biosens Bioelectron. 2007;22:1061–7.
27. Ding C, Zhao F, Ren R, Lin JM. An electrochemical biosensor for α-fetoprotein based on carbon paste electrode constructed of room temperature ionic liquid and gold nanoparticles. Talanta. 2009;78:1148–54.
28. Umasankar Y, Kumar SA, Chen S. Nanostructured materials for electrochemical biosensors. 1st ed. New York: Nova Science Publishers, Inc; 2009.
29. Lin X, Ni Y, Kokot S. Glassy carbon electrodes modified with gold nanoparticles for the simultaneous determination of three food antioxidant. Anal Chim Acta. 2013;765:54–62.
30. Huang H, Ran P, Liu Z. Impedance sensing of allergen–antibody interaction on glassy carbon electrode modified by gold electrodeposition. Bioelectrochemistry. 2007;70:257–62.
31. Ensafi AA, Amini M, Rezaei B, Talebi M. A novel diagnostic biosensor for distinguishing immunoglobulin mutated and unmutated types of chronic lymphocytic leukemia. Biosens Bioelectron. 2016;77:409–15.
32. Roushani M, Shahdost-fard F. Fabrication of an ultrasensitive ibuprofen nanoaptasensor based on covalent attachment of aptamer to electrochemically deposited gold nanoparticles on glassy carbon electrode. Talanta. 2015;144:510–6.
33. Haghshenas E, Madrakian T, Afkhami A. A novel electrochemical sensor based on magneto au nanoparticles/carbon paste electrode for voltammetric determination of acetaminophen in real samples. Mater Sci Eng C. 2015;57:205–14.
34. Santos CS, Mossanha R, Wohnrath K, Inaba J, Pessôa CA. Electrochemical immunosensor for qualitative diagnosis of the American trypanosomiasis based on gold modified with 3-Mercaptopropionic. J Electrochem Soc. 2016;163:158–62.
35. Yang Y, Tu Y, Wang X, Pan J, Ding Y. A label-free immunosensor for ultrasensitive detection of ketamine based on quartz crystal microbalance. Sensors. 2015;15:8540–9.
36. Manojlović NT, Mašković PZ, Vasiljević PJ, Jelić RM, Jusković MŽ, Sovrlić M, et al. HPLC analysis, antimicrobial and antioxidant activities of *Daphne cneorum* L. Hem Ind. 2012;66:709–16.

37. Rajesh, Sharma V, Mishra SK, Biradar AM. Synthesis and electrochemical characterization of myoglobin-antibody protein, immobilized self-assembled gold nanoparticles on ITO-glass plate. Mater Chem Phys. 2012;132:22–8.
38. Guoa Y, Guoa S, Fang Y, Dong S. Gold nanoparticle/carbon nanotube hybrids as an enhanced material for sensitive amperometric determination of tryptophan. Electrochim Acta. 2010;55:3927–31.
39. Lin J, He C, Zhang L, Zhang S. Sensitive amperometric immunosensor for a-fetoprotein based on carbon nanotube/gold nanoparticle doped chitosan film. Anal Biochem. 2009;384:130–5.
40. Cui R, Liu C, Shen J, Gao D, Zhu JJ, Chen HY. Gold nanoparticle–colloidal carbon nanosphere hybrid material: preparation, characterization, and application for an amplified electrochemical immunoassay. Adv Funct Mater. 2008;18:2197–204.
41. Favretto D, Piovan A, Filippini R, Caniato R. Monitoring the production yields of vincristine and vinblastine in *Catharanthus roseus* from somatic embryogenesis. Semiquantitative determination by flow-injection electrospray ionization mass spectrometry. Rapid Commun Mass Spectrom. 2001;15:364–9.